Reduction of Waste Smelter Slags using Top-Submerged Injection of Gaseous Reductants

Xiao-Yong Yan, Nan Li, Eric J Grimsey
Department of Minerals Engineering
and Extractive Metallurgy,
Western Australian School of Mines,
Curtin University of Technology,
PMB 22, Kalgoorlie 6430, Western Australia,
Australia, FAX 61 90 88 6181

ABSTRACT

The top-submerged injection method has been used to introduce methane and air mixtures into a waste smelter slag to reduce the dissolved nickel, cobalt and cuprous oxides. A number of parameters affecting the reduction rate have been investigated. These are total gas flowrate, methane to air ratio, temperature, slag composition, orifice size and immersion depth of the lance. The results show that the reduction is enhanced with increase in the methane-to-air ratio, and by using a smaller orifice and deeper immersion of the lance. The maximum metal reductions achieved were 90 percent for nickel, 70 percent for cobalt, and 55 percent for copper, with ten percent of the gas achieving equilibration with the slag under these conditions.

1. INTRODUCTION

Modern smelting processes are becoming progressively more intense through improved phase contact and the utilisation of oxygen enrichment. Higher smelting intensity leads to higher capacity smelters with lower capital costs, improved energy efficiency and improved materials handing. The conventional technology for non-ferrous smelting thus has moved from reverberatory smelting to flash smelting and now towards bath smelting. However, the amount of valuable metal lost in the waste slags has increased, through increased mechanical entrainment of the metal rich phase[1] and through increased chemical dissolution due to the higher oxygen potential being used in more intense processes[2]. Consequently, an intensive smelting process is usually followed by a slag cleaning step to provide for the chemical reduction of the dissolved metal oxides and for the settling of matte or metal phases from the slag.

The conventional process for slag cleaning involves the use of an auxiliary electric furnace charged with coke for reduction. This provides a quiescent environment for the settling and separation of matte and metal droplets from slag, but the rate of reduction is limited by the relatively poor contact between the coke and the slag, since the coke floats on the slag surface. The coupling of this relatively inefficient slag cleaning process with a modern intense smelting process is a technological mismatch and highlights the need for the development of more intense slag cleaning processes.

The opportunities for such a development lie firstly with processes which increase the rate of slag reduction and secondly with processes which enhance the coalescence of matte and metal droplets in the slag. There have been a number of attempts to develop more efficient slag cleaning processes[3-8], with one of the most effective methods being the injection of gaseous or solid reductants into the molten slag bath. During the injection, the reduction kinetics are improved significantly by the intense mixing of the reductants with the slag and the increased rates of heat and mass transfer[9-10]. Such injections may be carried out using the top-submerged lances, as utilised in the Sirosmelt/Ausmelt process[11-14].

The purpose of this work was to experimentally investigate the intensification of existing slag cleaning processes by the injection of methane and air mixtures using top-submerged lances, and to study the effects of total gas flowrate, methane-to-air ratio, temperature, slag composition, orifice size and immersion depth on the rate and extent of reduction. Since natural gas contains more than eighty percent methane, the results obtained in this study should be applicable to the reduction of slag with natural gas.

2. EXPERIMENTAL

2.1 Materials

Water-granulated nickel flash furnace slag was supplied by the Kalgoorlie Nickel Smelter of WMC Resources Ltd for the tests. The smelter operates with an appendage where the slag is reduced moderately by coke in the presence of carbon electrodes used for auxiliary heating. The slag is essentially an iron silicate which contains around six percent magnesia, three percent alumina and two percent of calcia. Nickel, copper and cobalt are present in the slag both as dissolved oxides and as entrained sulfides, with the relative amounts of each being determined by phase analysis using wet chemical methods (as developed at WMC Resources Ltd). The analysis of the master slag used in the experiments is given in Table I. The analysis for the starting slag of each

reduction test may vary slightly from this since it was based on the actual sample of slag used in the experiment.

Table I Typical composition of the slag used in the tests (in wt.%)

Fe (total) as FeO, $FeO_{1.5}$	42.0	Ni (total)*	0.38
SiO_2	29.5	NiO	0.42
MgO	6.6	Co (total)*	0.11
Al_2O_3	3.3	CoO	0.14
CaO	1.8	Cu (total)*	0.10
		$CuO_{1.5}$	0.09

* 10.5% of total Ni, 0% of total Co and 20% of total Cu were present as entrained sulfides.

Dried air and industrial grade methane (99.1 vol% CH_4; major impurity 0.6 vol% N_2) were used in the tests. Methane is burned with oxygen in the lance to form carbon monoxide and hydrogen gases prior to reduction according to the reaction:

$$CH_4 + 0.5\,O_2 \rightarrow CO + 2H_2$$

The stoichiometric ratio of methane-to-oxygen is 2:1 which represents a methane-to-air ratio of 0.43:1. Ratios greater than 0.43:1 will provide for the presence of fine carbon within the cracked gas.

2.2 Apparatus

The experimental setup used in the tests is shown in Fig.1. A magnesia crucible (55 mm (2.17 in.) outside diameter (O.D.), 51 mm (2.01 in.) inside diameter (I.D.) and 90 mm (3.54 in.) high) was covered with an alumina dish of 80 mm (3.15 in.) in diameter, and sealed with refractory cement. The dish had three holes and an alumina tube (15 mm (0.59 in.) O.D., 11 mm (0.43 in.) I.D., and 40 mm (1.58 in.) in length) was cemented into each hole to minimise slag spillage. A lance was immersed in the slag through the central hole of the dish. Other holes were used for temperature measurement and sampling. During a test the slag temperature was measured continuously using a type R thermocouple and displayed on a digital temperature indicator (DPM 24/40000).

The required methane-to-air ratio was established by adjusting the gas flowrates individually using micro-metering valves with the flowrates being monitored by calibrated mass flowmeters. A concentric, double alumina lance was used for the gas injection (Fig. 2). The lance consisted of an outside alumina sheath (8 mm (0.315 in.) O.D. and 5 mm (0.197 in.) I.D.) and an inside alumina tube (4 mm (0.157 in.) O.D. and 2 mm (0.078 in.) I.D.). A one or three millimetre hole was drilled as a nozzle at the end of the outside sheath.

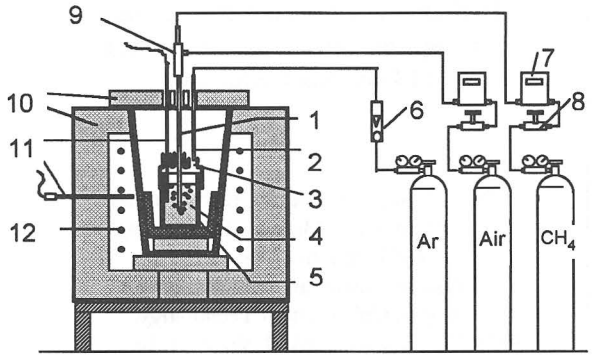

Fig. 1 A schematic of the experimental set-up used in the gaseous injection tests

1 - Alumina lance; 2 - Argon inlet; 3 - Slag sampling hole;
4 - Molten slag; 5 - Magnesia crucible (enlarged);
6 - Rotameter; 7 - Mass flow meter; 8 - Metering valve;
9 - Three-way connector; 10 - Insulation bricks;
11 - Type R thermocouples; 12 - Furnace heating elements.

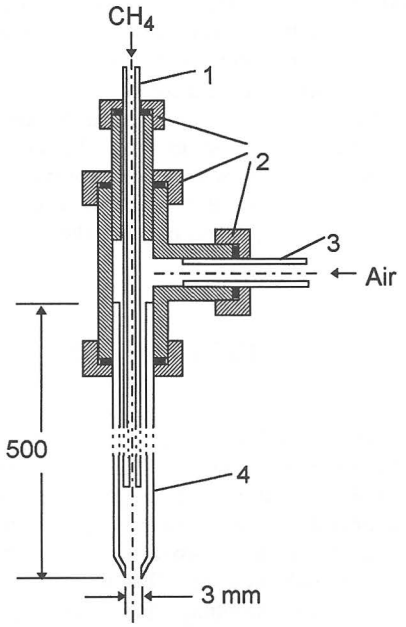

Fig. 2 Cross section of the double lance used in the tests.

1 - Inside alumina lance for methane (I.D. of 1.5 mm);
2 - Lock nuts with Teflon seals; 3 - Alumina tube;
4 - Outside alumina lance for air flow (I.D. of 5 mm).

Methane was delivered through the inside tube and air through the annulus. Both methane and air were pre-heated when they flowed through the hot lance, and they mixed and burned within ten millimetres below the opening of the inside tube. The best position for the opening of the inside tube was determined experimentally to be 100 mm (3.94 in.) above the nozzle. This provided sufficient space inside the lance for pre-combustion of methane with air prior to contact with the slag. The depth of lance immersion in the slag was 20 mm (0.79 in.) below the slag surface unless otherwise stated. In one test, pure carbon monoxide was used as a reductant, which was injected through the alumina sheath without the inside tube.

2.3 Procedure

The crucible was charged with 170 grams (5.99 oz) of slag and heated in the furnace under a cover of high purity argon. When the desirable temperature was reached, the molten slag was homogenised by bubbling high purity argon through an alumina lance for several minutes. The methane and air were then adjusted to provide the desired gas ratio and total flowrate, before the lance was lowered into the molten slag and the injection started. No attempt was made to collect the reduced metals into a discrete phase during the tests and the extent of metal oxide reduction was determined from slag samples collected at predetermined time intervals by freezing onto dipped stainless steel rods. The samples were dried, milled and analysed by wet chemical methods for their chemical and phase compositions. Each test lasted 50 minutes.

A series of tests were carried out also using 500 grams (17.61 oz) of slag in a larger magnesia crucible (63 mm (2.48 in.) O.D., 55 mm (2.17 in.) I.D., 140 mm (5.51 in.) high) to study the effects of the nozzle size and the lance immersion depth on the extent and rate of reduction. Tests were carried out using a 3 mm lance at 20 mm immersion, and a 1 mm lance at both 20 and 40 mm immersions.

3. RESULTS

3.1 Effect of total flowrate

Fig. 3 shows the influence of total gas flowrate (1, 2, 4 L/min) on the rate of reduction of nickel, cuprous and cobalt oxides at a methane-to-air ratio of 0.6 at 1573 K (2372 °F). It can be seen that a change in the total flowrate from 1 to 2 L/min (0.0353 or 0.0706 ft³/min) generally resulted in an enhancement in the reduction of nickel oxide but a further increase up to 4 L/min (0.141 ft³/min) had little beneficial effect. The behaviour of cobalt oxide was similar to that of nickel oxide, but there was little change in the reduction of cuprous oxide.

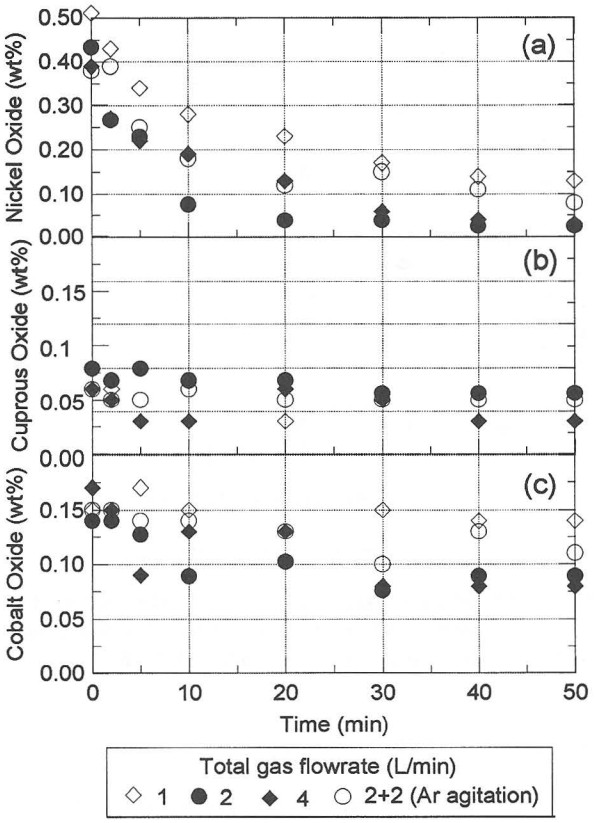

Fig. 3 Effect of total gas flowrate on the rates of reduction; Methane-to-air ratio: 0.6; Temperature: 1573 K.

Fig. 4 shows the extent of reduction of nickel and cobalt oxides, after the delivery of the same total volume of reducing gas (with methane-to-air ratio of 0.6 at 1573 K), but at three different flow rates, namely, for reduction after 10 minutes at 4 L/min, reduction after 20 minutes at 2 L/min, and reduction after 40 minutes at 1 L/min. The results indicate that under the present experimental arrangement, a flow rate of 2 L/min gave the most effective utilisation of reduction gas, and this flowrate was preferred for all subsequent testwork.

In one test (Fig. 3, open circle), an additional alumina lance (4 mm (0.257 in.) O.D. and 2 mm (0.0787 in.) I.D.) was used to inject high purity nitrogen at 2 L/min (0.0706 ft³/min) into the molten slag bath to provide for additional agitation of the slag bath during the injection of the reducing gas, also at 2 L/min (0.0706 ft³/min). The results indicate little difference compared to using the reducing gases alone at 2 L/min (0.0706 ft³/min).

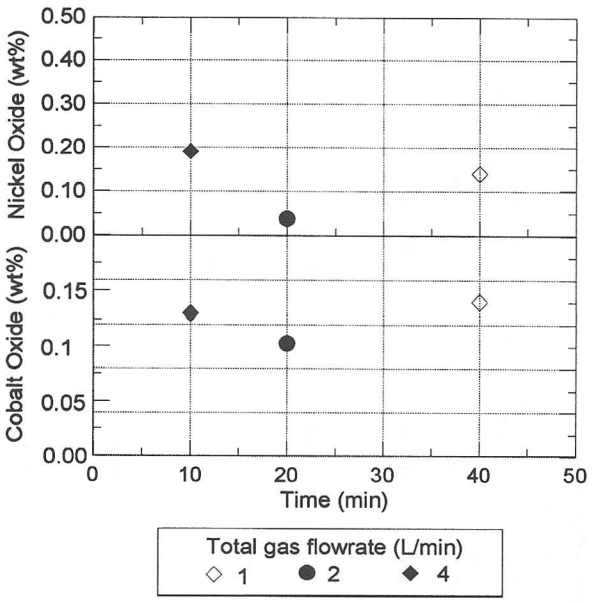

Fig. 4 The extent of reduction of nickel and cobalt oxides, after the delivery of the same total volume of reducing gas; Methane-to-air ratio: 0.6; Temperature: 1573 K.

3.2 Effect of methane-to-air ratio

Fig. 5 shows the rate of reduction of nickel, cuprous and cobalt oxides from slag at 1573 K (2372 °F) at various ratios of methane-to-air (0.43, 0.6, 0.8, 1.0) at a total flowrate of 2 L/min (0.0706 ft³/min). One test was conducted using pure carbon monoxide and is included for comparison. It can be seen that reduction was increased significantly for nickel and cobalt oxides after the methane-to-air ratio was increased from the stoichiometric ratio of 0.43:1, to 0.6:1, where free carbon is likely to be present in the gas; an increase from 0.6 to 1.0 provided further improvement in reduction only for cobalt oxide. Some improvement in the reduction of cuprous oxide was achieved with an increase in the methane-to-air ratio from 0.43 to 0.6 but the effect was not as pronounced as for nickel and cobalt; further reduction of copper was achieved also with an increase in the ratio to 1.0. Reduction using pure carbon monoxide was similar to that achieved using methane-to-air ratios of between 0.6 and 1.0 for all three oxides.

3.3 Effect of temperature

Fig. 6 shows the effect of an increase in bath temperature from 1573 to 1653 K (2372 to 2516 °F) on the oxide reduction rate. It appears that while an increase the temperature to 1653 K increases the initial rate of reduction, the level of reduction achieved after 50 minutes is less than at 1573 K.

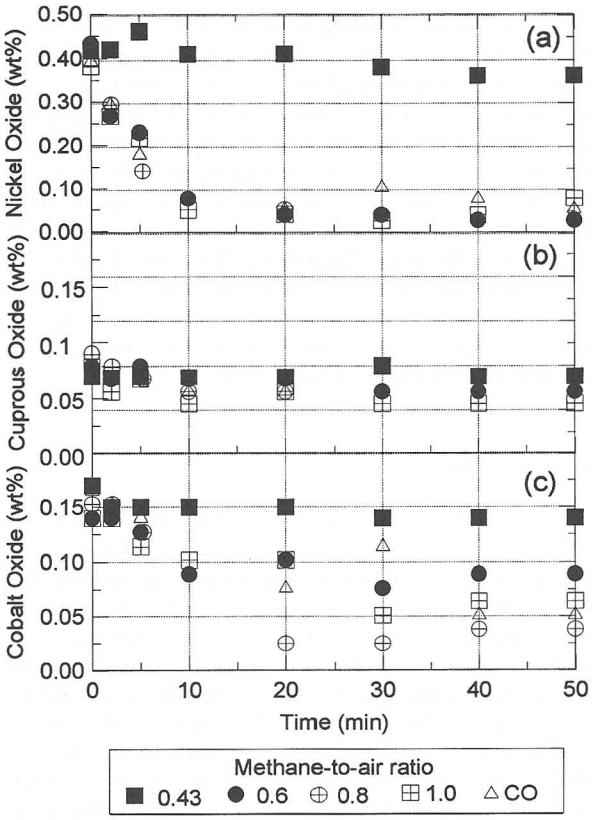

Fig. 5 Effect of methane-to-air ratio on the rates of reduction; Total gas flowrate:2L/min; Temperature:1573 K

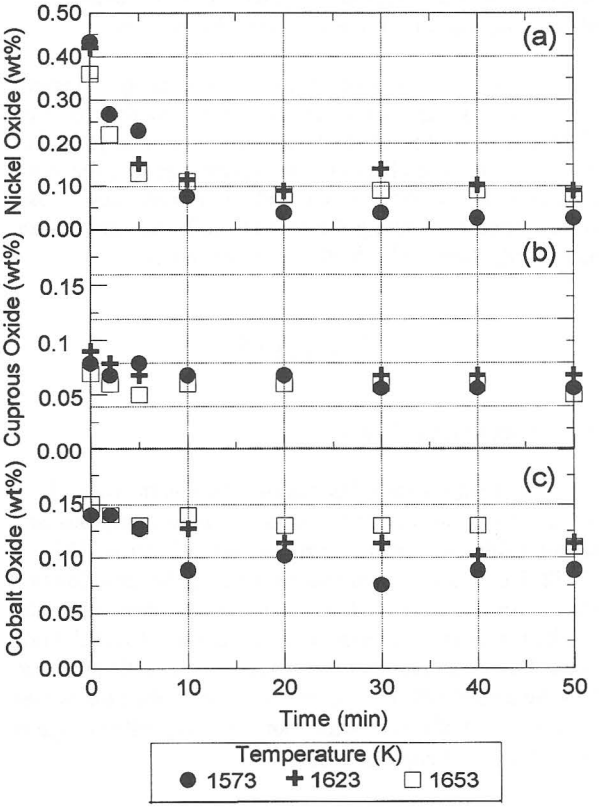

Fig. 6 Effect of temperature on the rate of reduction; Total gas flowrate: 2 L/min; Methane-to-air ratio: 0.6.

3.4 Effect of orifice size and immersion depth of the lance

Fig. 7 shows the influence of orifice size (3 and 1 mm) and immersion depth of the lance (20 or 40 mm) on the rate of reduction. Tests were conducted in a larger crucible using 500 grams of slag, compared to 170 grams in all other tests, and so the levels of reduction were lower than achieved with other tests under similar conditions (namely, 2 L/min and with a methane-to-air ratio of 0.6). The extent of reduction achieved for copper and cobalt oxides was insufficient to provide any clear trends above experimental scatter. However the data for nickel oxide reduction show that reduction was more effective using a smaller lance orifice at a greater depth.

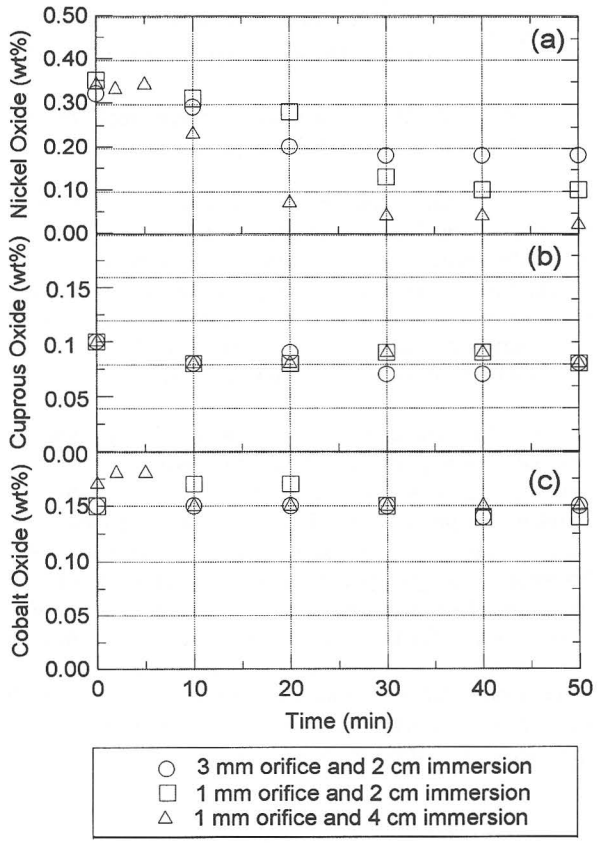

Fig. 7 Effect of the orifice size and immersion depth of the lance; Total gas flowrate: 2 L/min; Methane-to-air ratio: 0.6; Temperature: 1573 K; 500 g slag.

3.5 Effect of lime additions

Injection tests were conducted at a methane-to-air ratio of 1.0 and a total flowrate of 2 L/min (0.0706 ft^3/min) at 1573 K (2372 °F) with slags containing 1.8 weight percent lime (the base slag), 10.9 and 14.7 weight percent lime, and the effect on oxide reduction is shown in Fig. 8. It can be seen that an increase in lime content leads to an improvement in the reduction of all oxides, especially cobalt oxide.

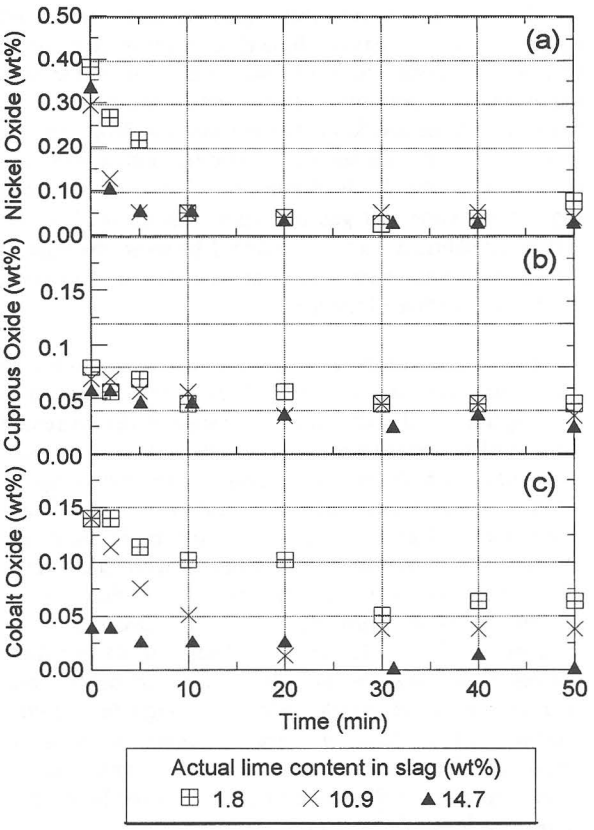

Fig. 8 Effect of lime additions on the rates of reduction; Total gas flowrate: 2 L/min; Methane-to-air ratio: 1.0; Temperature: 1573 K.

3. DISCUSSION

The interaction between the reducing gas bubbles and the slag is a very complex phenomenon. The reactive gas and slag species are brought to the gas-slag interface by the momentum created from the gas injection. The metal oxides are reduced by the gases at the interface and the products are transported away from the reaction sites. The bubbles rise through the slag and the bulk slag is mixed intensively during the injection; thus the movement of slag near the gas-slag boundary is rapid and it is likely that the rate controlling step would be the transport of gas to the gas/slag interface within the bubble. In this situation, chemical equilibrium may be achieved between gas and slag at the interface, but not necessarily for the bulk of gas within the bubble. Models based on these assumptions have been used successfully by other workers, notably

Robertson and co-workers[15], Mackey and Nagamori[16], and recently by Terry and Harris[17], to analyse gas/slag/metal interactions.

This work showed that agitation using secondary injection of an inert gas had little effect on reduction, which supports the assumption that mass transport in the bulk slag is not rate controlling. The extent of reduction from a fixed gas volume was found to vary with gas flow rate, and to increase with a decrease in nozzle (or bubble size) and an increase in the depth of injection. These observations support the view that gas utilisation was incomplete and that an equilibrium was not achieved between the bulk of the gas within the bubble and the slag, before the bubble reached the surface of the melt.

Gas utilisation should increase with a decrease in bubble size, not only because of the relative increase in gas/slag interfacial area but also because of the decreased path length for mass transport within the bubble. Much work has been carried out using water modelling to determine factors affecting bubble size from an orifice[18], where for a given gas/slag system and orifice size, the bubble size will decrease with increase in Reynolds number within the turbulent range. In this work, a flow rate of 2L/min was found to provide the best gas utilisation, compared to either 1 L/min or 4 L/min (Fig. 4), but these ambient flow rates are difficult to relate to bubble size, because the actual nozzle velocity at high temperature depends on the degree of preheat achieved in the lance, which will decrease with increase in flow rate; thus an increase in ambient flow rate will not necessarily result in an increase in nozzle flow rate.

Other effects observed in the tests may be rationalised in terms of thermodynamics. A increase in temperature decreases the equilibrium constants for the reduction of nickel, cobalt and copper oxides with either carbon monoxide or hydrogen[19] and this could account for the observed decrease in reduction with increase in temperature. Lime addition to iron silicate based slags increases the activity coefficients of nickel, cobalt and copper oxides and this may account for their improved reduction in the presence of lime. Finally, the significant enhancement in the reduction of oxides which was observed when the methane-to-air ratio was increased above the stoichiometric value of 0.43, to 0.6, indicated that with excess methane, the reduction was enhanced by the presence of highly reactive free carbon which could drive the reduction by reacting back with carbon dioxide through the Boudouard Reaction, namely:

$$CO_2 + C \rightarrow 2CO.$$

4. THERMODYNAMIC SIMULATION

A thermodynamic simulation was performed to estimate the percentage of the reducing gas used effectively in the reduction experiments. The stepwise model of Mackey and Nagamori[16] was utilised since this applies when the rate controlling step is mass transport in the gaseous phase. The model assumes that while a chemical equilibrium is achieved within a gas layer at the gas/slag interface, there is insufficient time for all of the gas within the bubble to reach the boundary and achieve equilibrium. The inefficiency is accounted for by the introduction of the term "degree of equilibrium attainment" (D_E), where:

$$D_E = \frac{\text{Moles of Gas Equilibrated with slag}}{\text{Total moles of Gas Injected into the Melt}}$$

The value of D_E is assumed independent of the composition of the slag to a first approximation.

The thermodynamic simulation is performed in series of steps. A small amount of gas mixture (methane and air) enters the reactor in each step, reaches equilibrium with the slag and then exits before more gas is added to the system in a new step. In this way, the continuous change in the composition of the slag, metal and gas phases can be simulated in a series of equilibrium calculations.

An ideal simulation would divide the total gas volume into bubble size portions and then progressively react these with the slag mass, releasing the gas after each reaction, to simulate the passage of a bubble through the melt. This would require a very large number of computations. Fortunately, in agreement with Mackey and Nagamori[16], it was found that such refinement is unnecessary, and that calculations performed once every 30 seconds at a flow of 2.0 L/min, gave very similar results to those calculated for much shorter times. The actual moles of gas used in each equilibrium step was calculated as a fraction of the total gas injected at 1 atmosphere pressure, according to:

$$\text{Moles (gas)} = D_E \frac{V}{RT} \frac{t}{60}$$

V is the gas flowrate in L/min, R is the gas constant (0.0821 L atm /mol /K), T is the ambient temperature in K, and t is the time for each step in seconds.

The calculation was carried out using a public domain, generic pyrometallurgical modeller called STEPSOL 3.0[20], which runs on an IBM PC and uses the Solgasmix algorithm of Eriksson to find the equilibrium composition for a given mass balance. The program requires an input of the species used to describe each phase, their free energies of formation, and the parameters for a model to describe

the activity behaviour of each condensed phase. Various model options are provided including the regular solution and the sub-regular three suffix Margules model. The gas phase is assumed to be ideal. The present system consists of a gas, a slag and a reduced metal product and details of their thermodynamic input data are given in Appendix A. The reduced metal product is finely dispersed within the slag and is assumed to be in equilibrium with it for the purposes of this calculation.

Figure 9 shows the experimental points for reduction at different methane-to-air ratios (cf Fig. 5), and the curves obtained from the simulation. The noticeable bumps on the curves were the result of performing the simulation at the experimentally recorded (variable) temperatures, rather than at the nominal constant temperature, of 1573 K in this case.

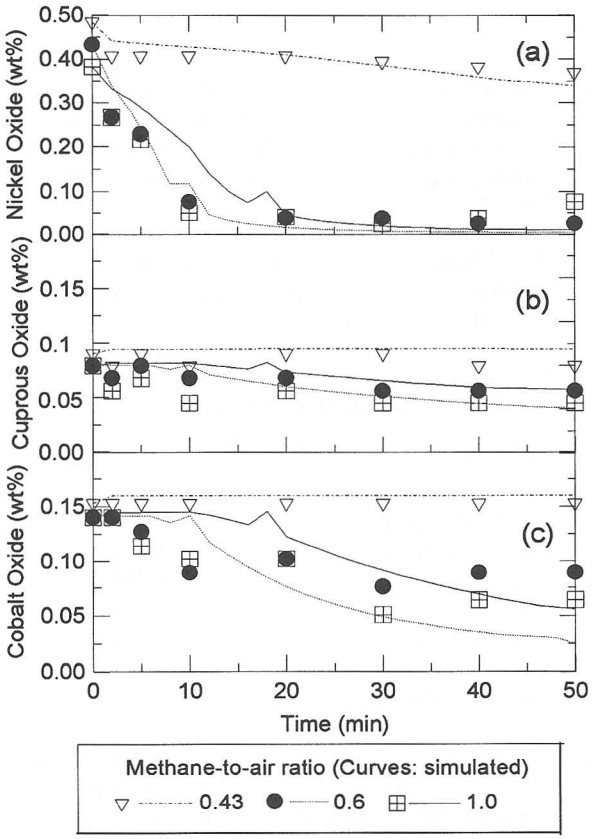

Fig. 9 Experimental data versus simulated curves of various methane to air ratio; Total gas flowrate of 2 L/min; Temperature: 1573 K. One percent of gas is assumed to be equilibrated for the ratio of 0.43 and ten percent for the ratios of 0.6 and 1.

The simulation for the stoichiometric methane-to-air ratio of 0.43 showed that only one percent of the gas had equilibrated with slag. However, when the ratio was increased to either 0.6 or 1.0, the equilibrated gas fraction increased to ten percent. At these above-stoichiometric ratios, free carbon will form in the gas. In order to complete the calculation, it was necessary to assume that the proportion of this carbon reacting with slag was the same as for the gaseous reductants, namely, carbon monoxide and hydrogen.

Figures 10 confirms that the data for reductions carried out at variable lime contents and at a methane-to-air ratio of 1.0 (cf Fig. 8) can be simulated also on the assumption of ten percent gas equilibration. The simulations of nickel oxide reduction shown in Figure 11, confirm that the percentage of gas equilibrating increases to 15 percent as the immersion depth increases from 20 to 40 mm and the nozzle size decreases from 3 to 1 mm in these tests.

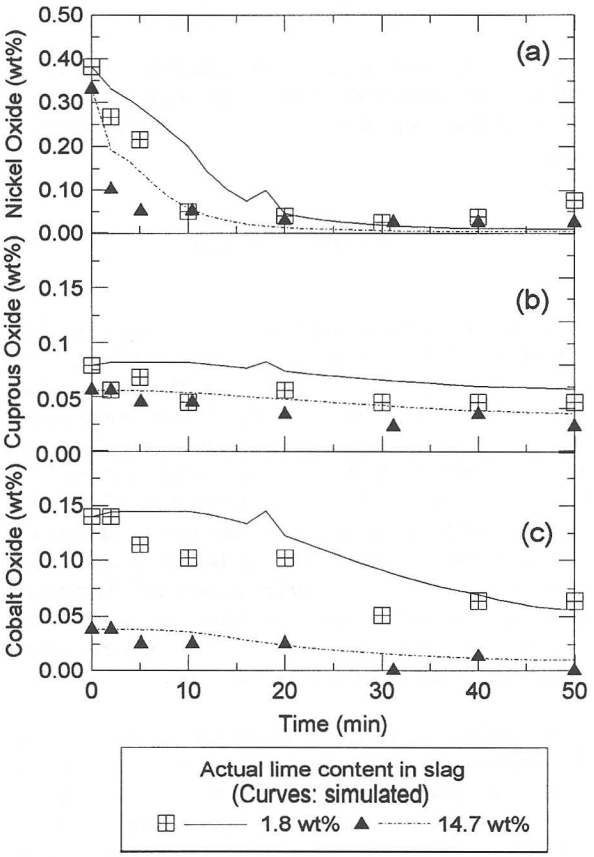

Fig. 10 Experimental data versus simulated curves of addition of lime; Total gas flowrate is 2 L/min; Methane to air ratio of 1.0; Temperature: 1573 K. Ten percent of gas is assumed to equilibrate in simulation.

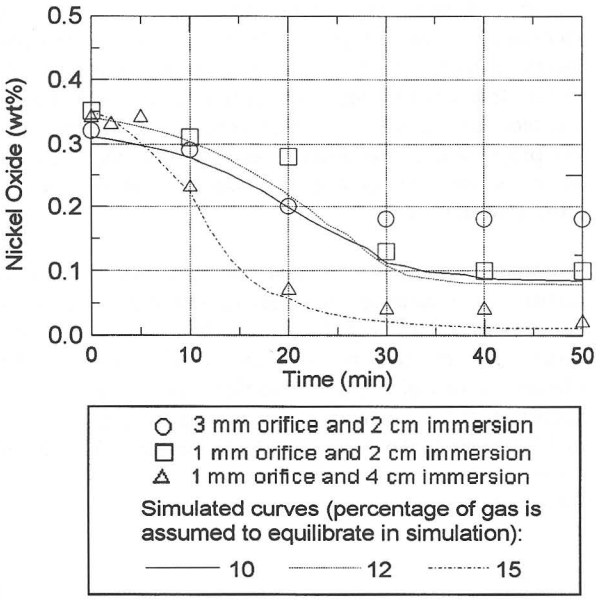

Fig. 11 Experimental data versus simulated curves of reduction of nickel oxide; Total gas flowrate: 2 L/min; Methane-to-air ratio: 0.6; Temperature: 1573 K; 500 g slag.

5. CONCLUSIONS

A nickel flash furnace waste slag, containing around 0.4 percent nickel oxide and 0.1 percent each of cobalt and copper oxides, was injected with methane and air mixtures mainly at 1573 K in laboratory experiments. Reduction of up to 90 percent nickel oxide, 70 percent of cobalt oxide and 55 percent of cuprous oxide was achieved at methane-to-air ratios between 0.6 to 1.0, while minimal reduction was achieved at the stoichiometric methane to air ratio (for CO and H_2 formation) of 0.43. An increase in temperature from 1573 to 1653 K, had a minimal, although detrimental, effect on the extent of reduction, while increasing the lime content of slag from around 2 to 15 percent enhanced the reduction, especially for nickel oxide.

A thermodynamic simulation model was used to calculate the percent of the input gas which equilibrated with slag, on the assumption that mass transfer within the gas bubbles was rate controlling under the experimental conditions. Ten percent of gas was found to equilibrate with slag for methane-to-air ratios of 0.6 to 1.0, with the percentage increasing to 15 with a decrease in the lance orifice size (from 3 to 1 mm) and an increase in the lance immersion depth (from 20 to 40 mm). These observations support the view that mass transport in the gas phase was rate controlling and that the extent of gas equilibration (and utilisation) in practice would very much depend on the fluid dynamics of the injection system.

ACKNOWLEDGMENTS

The authors gratefully acknowledge the Australian Research Council and WMC Resources Ltd. for their financial support of this project. We also wish to express our appreciation to Mr B. J. Elliot of the WMC Kalgoorlie Nickel Smelter for his encouragement and strong interest, Dr. A. Warczok of the University of Toronto for his advice and the chemists at the assay laboratory of the Kalgoorlie Nickel Smelter for the chemical analysis of all the slag samples.

REFERENCES

1. J.M. Floyd and P.J. Mackey, "Developments in the Pyrometallurgical Treatment of Slag: A Review of Current Technology and Physical Chemistry", IMM Symp. Extractive Met.'81, IMM, London, 1981, pp. 345-371.

2. P.J. Mackey, "The Physical Chemistry of Copper Smelting Slags - A Review", Can. Met. Quart., Vol. 21, 1982, pp. 221-260.

3. C.C. Banks and D.A. Harrison, "The Recovery of Non-Ferrous Metals from Secondary Copper smelter Discard Slags", Can. Met. Quart., Vol. 14, 1975, pp. 183-190.

4. S.C.C. Barnett and J.H.E. Jeffes, "Recovery of Nickel from Thompson Smelter Electric Furnace Slag", Trans. IMM, Vol. 86, 1977, pp. C155-C157.

5. P.R. Ammann, J.J. Kim, and T.A. Loose, "The Kennecott Process for Nickel-Slag Cleaning", J. Met., Feb. 1979, pp. 20-25.

6. O. Addemir, J. Steinhauser, and W. Wuth, "Copper and Cobalt Recovery from Slags by Top-Injection of Different Solid Reductants", Trans. IMM., Vol. 95, 1986, pp. C149-155.

7. Y. Mori and T. Kimura, "Cleaning of Copper Converter Slag by Coal Injection", Met. Review MMIJ, Vol. 3, No. 3, 1986, pp. 141-154.

8. W.R.N. Snelgrove and J.C. Taylor, "The Recovery of Values from Non-Ferrous Smelter Slags", Can. Met. Quart., Vol. 20, 1981, pp. 231-240.

9. J.M. Floyd and D.S. Conochie, "SIROSMELT - The First Ten Years", Symp. "Extractive Metall., AusIMM, Melbourne, Australia, 1984, pp. 1-8.

10. J.M. Floyd, "Submerged Bath Smelting Applied to the Non-Ferrous Metal Industry", Paul E. Queneau Int. Symp. Extractive Metall. Copper, Nickel and Cobalt, TMS, Vol. I, 1993, pp. 473-487.

11. J.M. Floyd, "Nickel Slag Cleaning", Can. patent No. 998246, 1976.

12. J. M. Floyd, G. J. Leahy, R. L. Player, and D. J. Wright, "Submerged Combustion Technology Applied to Copper Slag Treatment", AusIMM Operators Conf., North Queensland, Australia, 1978, pp. 323-327.

13. J.M. Floyd and D.S. Conochie, "Reduction of Liquid Tin Smelting Slags: 2 - Development of Submerged Combustion Process", Trans. IMM, Vol. 88, 1979, pp. C123-C128.

14. J.M. Flody and D.S. Conochie, "Reduction of Liquid Tin Smelting Slags: 1 - Laboratory Investigations", Trans. IMM, Vol. 88, 1979, pp. C114-122.

15. D.G.C. Robertson, B. Deo, and S. Ohguchi, "Multicomponent Mixed-Transport-Control Theory for Kinetics of Coupled Slag/Metal and Slag/Metal/Gas Reactions: Application to Desulphurization of Molten Iron", Iron and Steelmaking, Vol. 11, 1984, pp. 41-55.

16. P.J. Mackey and M. Nagamori, "Stepwise Equilibrium Simulation of Zinc Fuming from Reverberatory Slag with CO Gas", H.H. Kellogg Int. Symp. Quantitative Description of Met. Extn Processes, TMS, 1991, pp. 111-125.

17. B.S. Terry and C.L. Harris, "Kinetics of Reduction of Metal Values from Fayalite-Based Slags - Part 2: Modelling of Idealised Slag-Cleaning Conditions", Trans. IMM., Vol. 104, 1995, pp. C92-C101.

18. J. Szekely, N.J. Themelis, Rate Phenomena in Process Metallurgy, Wiley-Interscience, 1971.

19. O. Kubaschewski, E.L. Evans and C.B. Alcock, Metallurgical Thermochemistry, Pergamon, 5th ed., 1979.

20. E.J. Grimsey and A.E. Morris, "Activity Models for Pyrometallurgical Processes Using STEPSOL", AusIMM Ext. Met. Conf., Perth, Australia, 1991, pp. 257-261.

21. H.H. Kellogg, "Thermochemistry of Nickel-Matte Converting", Can. Met. Quart.,Vol 26, 1987, pp. 285-298.

22. R.P. Goel and H.H. Kellogg, "Mathematical Description of the Thermochemical Properties of Iron Silicate Slags Containing Cu_2O and/or CaO", Unpublished Report.

23. E.J. Grimsey and J. M. Toguri, "Cobalt in Iron Silicate Slags", Can. Met. Quart., Vol 27, 1988, pp. 331-333.

24. J.M. Larrain, "High Temperature Thermodynamic Properties of Iron Nickel Alloys", CALPHAD, Vol. 4, 1980, pp. 155-171.

25. P. Wu, private communication, 1995.

26. R.C. Sharma, "Thermodynamic Analysis of Cu-Ni System", Indian Inst.Met., Vol 35, 1982, pp. 372-375.

27. Y. Chuang, R. Schmid, and Y. Austin Chang, "Thermodynamic Analysis of the Iron-Copper System 1: The Stable and Metastable Phase Equilibria", Met Trans A, Vol 15A, 1984, pp. 1921-1930.

APPENDIX A

Table A1: A list of species and free energy coefficients used in STEPSOL modelling

Species:	**Gas**	N2, CO, CO_2, H_2, H_2O, O_2, CH_4			
	Slag	FeO (hl), $FeO_{1.5}$ (hl), Fe (l), SiO_2 (hl), CaO (hl), MgO (l), Al_2O_3 (l), Ca_2SiO_4 (hl), NiO (hl), Ni (l), CoO (s)			
	Alloy	Fe (s), Ni (s), $FeNi_3$ (s), Cu (s), Co (s)			
Free Energy Coefficients	**Species**	**a**	**b**	**c**	**Source**
Gas	**N_2**	0	0	0	
	CO	-24596	1.92566	-36.522	1
	CO_2	-93513	0.67301	-5.7231	1
	H_2	0	0	0	
	H_2O	-57570	1.54908	0.83876	1
	O_2	0	0	0	
	CH_4	-22494	-0.18598	28.2932	1
Slag	**FeO**	-58564	0	12.6708	2
	$FeO_{1.5}$ (hl)	-88906	0	25.6039	2
	Fe (l)	0	0	0	
	SiO_2 (hl)	11863	0	-1.9248	2
	CaO (hl)	6452	0	-1.3467	2
	MgO (l)	0	0	0	
	Al_2O_3 (l)	0	0	0	
	Ca_2SiO_4 (hl)	-9294	0	-8.9168	2
	NiO (hl)	-43775	-0.0442	17.3382	2
	Ni (l)	0	0	0	
	$CuO_{0.5}$ (l)	-20718	0	9.25	3
	CoO (s)	-59570	0	18.92	4
Alloy	**Fe (s)**	-3645	0	2.014	2
	Ni (s)	-1324	1.65	-11.534	2
	$FeNi_3$ (s)	-13975	4.95	-30.65	5
	Cu (s)	-3100	0	2.286	6
	Co (s)	-3870	0	2.188	6

Note: symbols l, hl, and s in brackets denote liquid, hypothetical liquid and solid, respectively. All free energies were calculated from the formula: $\Delta G^o_T = a + bTlnT+cT$ cal/mol. Standard states are pure liquid metals, SiO_2(s), and CaO(s).

Sources: 1. JANAF 3rd Ed. provided by the STEPSOL database FREED; 2. Kellogg[21]. 3. Kellogg and Goel[22]; 4. Grimsey and Toguri[23]; 5. Larrian[24]; 6. Kalsaschewsi et al.[19].

Table A2: Three suffix Margules constants (C_{ij}) for slag species

i / j	FeO	$FeO_{1.5}$(hl)	Fe(l)	SiO_2(hl)	CaO(hl)	Ca_2SiO_4(hl)	NiO(hl)	Ni(l)	$CuO_{0.5}$(l)
FeO	0	-2461	9199	-11115	115	-129	-1200	9000	2750
$FeO_{1.5}$(hl)	-1173	0	9882	-455	-7655	-5270	-1000	9000	4600
Fe(l)	7188	9882	0	7376	8242	7376	8000	590	8000
SiO_2(hl)	-4165	-147	7376	0	-18700	-13614	-5000	9000	-4700
CaO(hl)	115	-7655	8242	-29000	0	-344	-3800	9000	4000
Ca_2SiO_4(hl)	-129	-5270	7376	-13614	-344	0	-1800	9000	2000
NiO(hl)	-1100	-1000	8000	-4700	-4000	-1200	0	8271	0
Ni(l)	9000	9000	-1380	9000	9000	9000	-15911	0	0
$CuO_{0.5}$(l)	4200	-700	8000	-5100	4900	-22000	0	0	0

Note: The three suffix Margules parameters, h_{ij}, are calculated from the equation: $h_{ij} = C_{ij}/T + D_{ij}$. The above table lists values of C_{ij}, all D_{ij} are zero except for $D_{Ni\text{-}NiO} = 6.5643$ and $D_{NiO\text{-}Ni} = -2.192$. Sources: Kellogg[21] except for $CuO_{0.5}$ from Kellogg and Goel[22]. Activity coefficients of Al_2O_3(l) and MgO(l) set to 0.04 and 0.09 as a first approximation (data estimated from quasi-chemical model)[25]; activity coefficient of CoO (s) set to 2.0[23].

Table A3: Three suffix Margules constants (C_{ij} and D_{ij}) for alloy species

C_{ij}	i / j	Fe(s)	Ni(s)	$FeNi_3$(l)	Cu(s)
	Fe(s)	0	100	-2380	6923.87
	Ni(s)	-1160	0	-590	300
	$FeNi_3$(l)	-2380	-590	0	0
	Cu(s)	4955.52	1400	0	0
D_{ij}	**i / j**	**Fe(s)**	**Ni(s)**	**$FeNi_3$(l)**	**Cu(s)**
	Fe(s)	0	0	0	-1.7363
	Ni(s)	0	0	0	0.57658
	$FeNi_3$(l)	0	0	0	0
	Cu(s)	-0.68933	0.00166	0	0

Parameters for the Ni-Fe system are from Larrain[24]. Parameters for the Cu-Ni and Fe-Cu binaries have been calculated using the respective binary data of Sharma[26] and Chuang et al.[27], where $h_{ij} = C_{ij}/T + D_{ij} = \ln \gamma^0_i$, that is, the three suffix Margules parameters are estimated from the logarithm of the infinite dilution activity coefficients for the respective binaries. The Fe-Co, Ni-Co and Co-Cu systems are close to ideal, and thus their respective interaction parameters, not shown in the table, have been set to zero.